Asian Journal of Andrology (2018) 20, 313–315
www.asiaandro.com; www.ajandrology.com

Open Access

LETTER TO THE EDITOR

Prostate Disease

MRI feature analysis of uncommon prostatic malignant tumors

Zhao-Yan Feng, Xiang-De Min, Liang Wang, Ba-Sen Li, Zan Ke, Pei-Pei Zhang, Zhen Kang

Asian Journal of Andrology (2018) **20**, 313–315; doi: 10.4103/aja.aja_12_17; published online: 30 May 2017

Dear Editor,

Most prostatic neoplasms are epithelial in origin. Non-epithelial prostatic neoplasms are quite rare, but they cover a broad array of types that include neuroendocrine tumors, mesenchymal tumors, hematolymphoid tumors, miscellaneous tumors, etc.[1,2] Unlike prostate cancer, there is no specific serum marker for non-epithelial prostatic neoplasms at present, and the majority of patients present with a large pelvic mass and compressive symptoms of dysuria or abdominal pain. Imaging plays an important role in the investigation of prostate masses, although transrectal ultrasound-guided prostate biopsy remains the gold standard for diagnosis. Magnetic resonance imaging (MRI) contributes to determining the site of origin of the tumor, local extent, and signal characteristics owing to its high soft-tissue contrast resolution. Many studies have demonstrated that MRI characteristics can help predict histological types of tumors, which can guide clinical treatment.[3–5] As there is a low morbidity rate for uncommon prostatic neoplasms, MRI features have rarely been described in the literature and they are mainly reported as case reports.[6–8] In this letter, we retrospectively reviewed the MRI features of 15 cases of uncommon prostatic malignant tumors, which, to our knowledge, is the largest number of these tumors reported to assess MRI features. As accurate diagnosis is critical for appropriate clinical workup and management, the aim of this study was to explore some salient MRI characteristics of uncommon prostatic malignant tumors to improve understanding and facilitate the differential diagnosis.

This retrospective study was approved by Tongji Hospital, Tongji Medical College, Huzhong University of Science and Technology Institutional Review Board. We collected the clinical data of 15 cases of uncommon prostatic tumor patients from January 1, 2011, to December 31, 2015, in Tongji Hospital. And informed consents were obtained from all patients. The age range was from 22 years to 69 years, with a median age of 46 years. Nine cases presented with dysuria, two cases had lower abdominal pain, two cases were accidentally discovered on routine physical examination, one case had dyschezia as well as fresh blood in the feces, and one case had waist pain as well as perineal pain. The median value of the serum prostate-specific antigen (PSA) was 1.412 (range: 0.435–126.634) ng ml^{-1}. The pathological study was performed via transrectal ultrasound-guided biopsy in 11 patients, transurethral resection of the prostate in one patient, and open surgery in three patients. The final pathological diagnoses were embryonal rhabdomyosarcoma (RMS) in two patients, prostatic stromal sarcoma (PSS) in four, mesenchymal tumors not-otherwise-specified in four, small cell carcinoma (SCC) in three, and lymphoma in two. All the patients underwent conventional MRI including T1-weighted imaging (T1WI) and T2-weighted imaging (T2WI), nine patients underwent diffusion-weighted imaging (DWI), and ten patients underwent dynamic contrast-enhanced (DCE) MRI. The clinical characteristics and MRI findings are shown in **Table 1**. The detailed clinical, immunohistochemical, and MRI information are shown in **Supplementary Table 1–3**. Tumors were round ($n = 3$), lobular ($n = 6$), and irregular ($n = 6$). Eleven tumors occupied the entire prostate, with loss of the normal zonal anatomy on T2-weighted images. Four tumors occupied the majority of the prostate. Among the nine patients who had DWI examinations, all tumors showed high signal and the apparent diffusion coefficient value was relatively low. A typical case of embryonal rhabdomyosarcoma is shown in **Figure 1**. The tumor presented with a well-defined T2 low signal pseudocapsule with internal cystic degeneration, bleeding, large necrotic areas and exerted a significant mass effect on bladder and rectum.

For the ten prostatic malignant mesenchymal tumors, tumors had low signals mixed with patchy high signals ($n = 5$) and were isointense ($n = 5$) on T1WI. Most prostate sarcomas had heterogeneous signal intensity on T2WI, which was consistent with multiple cysts (8/10), hemorrhagic necrosis (7/10) as well as marked heterogeneous enhancement (6/6) after the administration of contrast agents. Most of the prostate sarcomas (9/10) presented with a well-defined T2 low signal pseudocapsule and exerted a significant mass effect on adjacent structures, such as bladder ($n = 5$) and rectum ($n = 5$). There was evidence of adjacent invasion of the seminal vesicle ($n = 8$), bladder ($n = 2$), and rectum ($n = 3$). There was evidence of distant metastatic spread (lung metastasis in two cases and liver metastasis in one case). For the three small-cell carcinomas, T2WI showed a large heterogeneous prostatic mass and the prostate capsule was incomplete. The lesions were isointense on T1WI and mildly hyperintense on T2WI. The lesions showed mild or moderate heterogeneous enhancement after the administration of a contrast agent. Some cases showed invasion of adjacent structures, which showed involvement of the seminal vesicle ($n = 3$), bladder ($n = 3$), and rectum ($n = 2$). Pelvis lymph node metastasis was present in one case. There was evidence of distant metastasis in one (liver) case and two (bone) cases. For the two B-cell non-Hodgkin lymphomas, one case was predominantly in the prostate

The Department of Radiology, Tongji Hospital, Tongji Medical College, Huazhong University of Science and Technology, Wuhan 430030, China.
Correspondence: Dr. L Wang (wang6@tjh.tjmu.edu.cn)
Received: 17 November 2016; Accepted: 15 March 2017

Table 1: The clinical characteristics and magnetic resonance imaging findings

Number of patients	*Age (year)*	*Histology*	*PSA (ng ml^{-1})*	*Shape*	*T2WI*	*T1WI*	*DWI*	*Pseudocapsule*	*Cystic change*	*Necrosis*	*Adjacent invasion*
1	43	Embryonal rhabdomyosarcoma	0.655	Irregular	Hyper Iso	Iso Hyper	Hyper	Present	Present	Present	Seminal vesicle invasion, bladder and rectal compression
2	22	Embryonal rhabdomyosarcoma	1.668	Lobular	Hyper	Iso Hyper	Hyper	Present	Present	Present	Involving the penis and the right obturator muscle, bladder compression, seminal vesicle intact
3	25	Stromal sarcoma	0.471	Lobular	Hyper	Iso Hyper	Hyper	Present	Present	Present	Seminal vesicle invasion, bladder rectal compression
4	64	Stromal sarcoma	1.937	Lobular	Hyper	Iso	-	Present	Present	Absent	Seminal vesicle invasion, bladder rectal compression
5	45	Stromal sarcoma	2.500	Round	Hype Iso	Iso	-	Present	Present	Present	Seminal vesicle invasion, rectal compression
6	67	Stromal sarcoma	0.970	Lobular	Hyper	Iso	-	Present	Present	Absent	Seminal vesicle intact, rectal compression
7	46	Malignant mesenchymal tumors	0.435	Irregular	Hyper	Iso	-	Present	Present	Absent	Seminal vesicle, rectal and bladder invasion, retroperitoneal nodes metastatic
8	43	Malignant mesenchymal tumors	1.020	Lobular	Hyper	Iso	-	Present	Present	Present	Seminal vesicle invasion
9	25	Low-grade sarcoma	2.630	Irregular	Hyper Hypo	Iso hyper	Hyper	Present	Present	Present	Seminal vesicle, rectal and bladder invasion
10	34	Spindle cell sarcoma	1.412	Lobular	Hype Iso	Iso Hyper	Hyper	Absent	Present	Present	Seminal vesicle invasion, bladder compression, rectal invasion
11	63	Small cell carcinoma	5.600	Round	Hype Hypo	Hypo Hyper	-	Absent	Absent	Present	Seminal vesicle and bladder invasion
12	69	Small cell carcinoma	3.140	Irregular	Hyper	Hypo Hyper	Hyper	Absent	Present	Present	Seminal vesicle, rectal and bladder invasion
13	64	Small cell carcinoma	126.634	Irregular	Hype Hypo	Iso	Hyper	Absent	Absent	Present	Seminal vesicle and bladder invasion, pelvis lymph node metastasis, rectal invasion maybe
14	50	Diffuse large B-cell lymphoma	0.522	Irregular	Iso	Iso	Hyper	Absent	Absent	Absent	Seminal vesicle, rectal and bladder invasion, pelvis lymph node metastasis
15	57	Follicular lymphoma	0.839	Round	Iso	Iso	Hyper	Absent	Absent	Absent	Seminal vesicle and bladder invasion, pelvis lymph node metastasis

MRI: magnetic resonance imaging; PSA: prostate specific antigen; Hyper: hyperintense; Iso: isointense; Hypo: hypointense; -: none; T2WI: T2-weighted imaging; T1WI: T1-weighted imaging; DWI: diffusion-weighted imaging

and one case extended to adjacent tissues. The tumors were found to be homogeneously isointense on T1WI and homogeneously isointense on T2WI. Both cases underwent dynamic contrast-enhanced scans and demonstrated moderate and homogeneous enhancement. All of the cases had nodal involvement. One case showed multiple enlarged pelvis and retroperitoneal nodes. Adjacent involvement included the seminal vesicle ($n = 2$), bladder ($n = 2$), and rectum ($n = 1$). There was no clinical or radiologic evidence of distant metastasis in any patients.

Noninvasive multiparametric MRI provides comprehensive information that is needed for preoperative diagnosis and evaluation of prostate neoplasms. By combining the clinical finding and imaging, it is possible to primarily differentiate the histologic subtypes of prostate neoplasms. First, it is essential to distinguish uncommon prostatic malignant tumors from prostate adenocarcinoma because of their differences in management and prognoses. Prostate cancer tends to occur at an older age after 50 years, while some malignant mesenchymal tumors such as RMS are more common in children and young adults.[6] Most prostate cancer cases are asymptomatic and are detected by PSA screening. However, the uncommon prostatic malignant tumors including RMS, stromal tumors, and lymphomas are presented with obstructive urinary symptoms and total serum PSA levels in the normal range. On MRI, most cases are found to have malignant enlargement of the prostate, with loss of the normal zonal anatomy, whereas prostate cancer more often shows homogeneous hypointense masses on T2WI. Second, several features may help differentiate the histologic subtypes of uncommon prostatic malignant tumors. Most of the malignant mesenchymal tumors, such as RMS and PSS, demonstrate a well-defined and low signal intensity pseudocapsule. Cystic components are visualized.[9] In contrast to the mesenchymal tumors, neuroendocrine SCC is characterized by regional nodal invasion, adjacent involvement, and distant metastasis. Hemorrhage and necrosis are very common because of high malignancy and rapid growth and there is no pseudocapsule. Serum neuron-specific enolase values and serum PSA is always elevated.[10,11] The typical characteristics of prostate lymphoma are that tumors are homogeneously isointense on T1WI and homogeneously isointense on T2WI, and rarely have hemorrhage and necrosis. Tumors are moderately and homogeneously enhanced after gadolinium injection.[12]

In conclusion, we found some differences among RMS, PSS, SCC, and lymphoma, although there was some overlap in the MR imaging findings. Combined with clinical and laboratory indicators, MRI can provide a credible preoperative diagnosis, avoiding the provision of unnecessary clinical testing or therapies to patients.

AUTHOR CONTRIBUTIONS

ZYF and LW participated in the study conception and design, data analysis and interpretation, and manuscript drafting. XDM participated in the paper's discussion. ZK (Zan Ke) and PPZ helped collect the clinical data. LW, BSL, and ZK (Zhen Kang) reviewed and edited the manuscript. All authors read and approved the final manuscript.

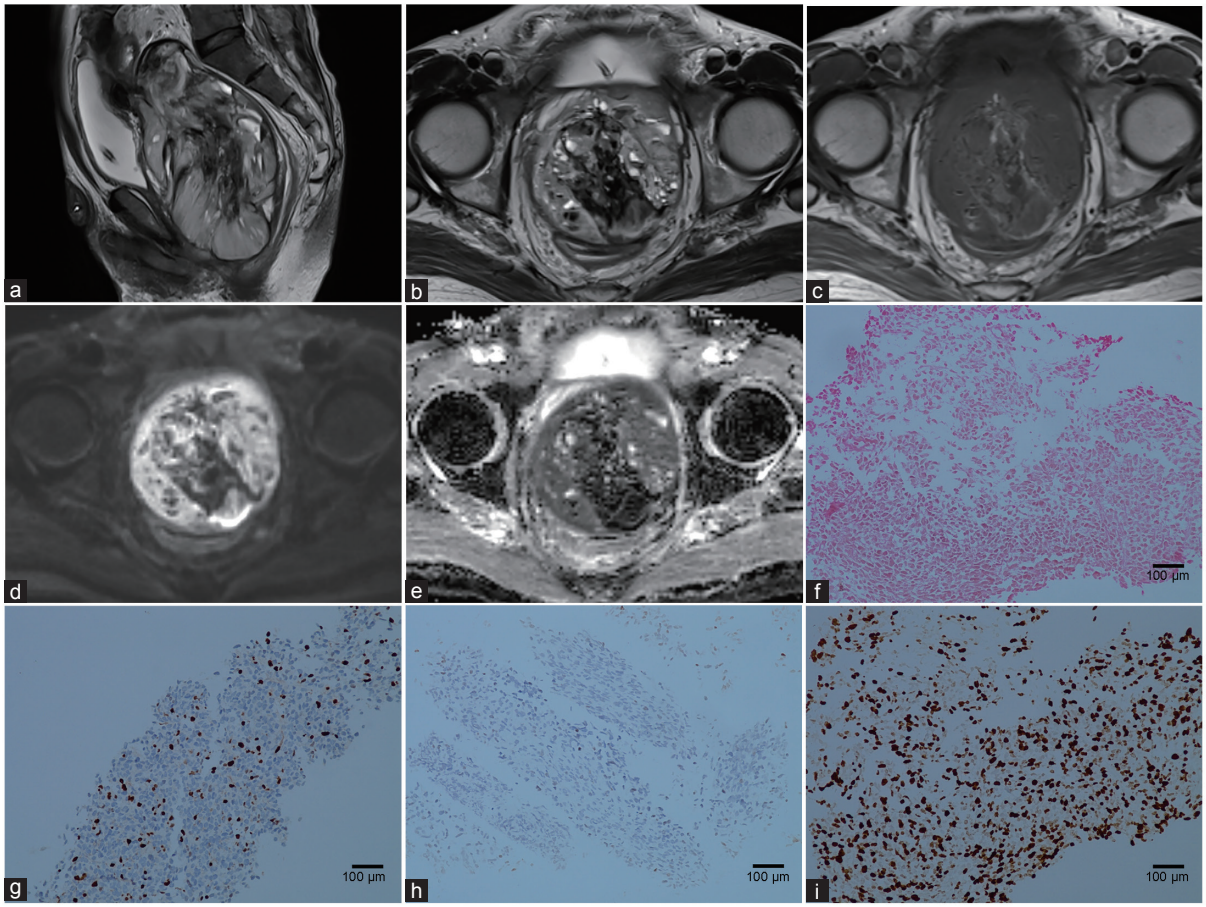

Figure 1: A 43-year-old man with embryonal rhabdomyosarcoma. (**a**) A large well-defined and heterogeneous mass invaded the entire prostate with compression of the urinary bladder and rectum on sagittal T2WI. (**b**) The tumor revealed heterogeneous signal intensity with internal cystic degeneration, bleeding, and large necrotic areas on axial T2WI. (**c**) The tumor revealed isointense signals, containing areas of high signal compatible with hemorrhage on T1WI. (**d**) DWI with a b value (diffusion-sensitized gradient) of 1000 s mm^{-2}, (**e**) the solid part of the tumors demonstrated restricted diffusion and a low apparent diffusion coefficient value. (**f**) Light microscopic examination for biopsy (HE staining magnification, 200×). Immunohistochemical studies showed that the neoplastic cells were positive for (**g**) Myogenin, (**h**) MyoD1 and (**i**) Ki-67 LI 60%. Scale bars = 100 μm. T2WI: T2-weighted imaging; T1WI: T1-weighted imaging; DWI: diffusion-weighted imaging; HE: hematoxylin-eosin.

COMPETING INTERESTS

All authors declare no competing interests.

ACKNOWLEDGMENTS

This study was supported by the grant from the National Natural Science Foundation of China (No. 81671656, 81171307).

Supplementary information is linked to the online version of the paper on the *Asian Journal of Andrology* website.

REFERENCES

1 Paner GP, Aron M, Hansel DE, Amin MB. Non-epithelial neoplasms of the prostate. *Histopathology* 2012; 60: 166–86.
2 Humphrey PA, Moch H, Cubilla AL, Ulbright TM, Reuter VE. The 2016 WHO classification of tumours of the urinary system and male genital organs – Part B: Prostate and bladder tumours. *Eur Urol* 2016; 70: 106–19.
3 Liu LP, Zhang XX, Cui LB, Li J, Yang JL, *et al*. Preliminary comparison of diffusion-weighted MRI and PET/CT in predicting histological type and malignancy of lung cancer. *Clin Respir J* 2015; 11: 151–8.
4 Koob M, Girard N, Ghattas B, Fellah S, Confort-Gouny S, *et al*. The diagnostic accuracy of multiparametric MRI to determine pediatric brain tumor grades and types. *J Neurooncol* 2016; 127: 345–53.
5 Ma L, Xu X, Zhang M, Zheng S, Zhang B, *et al*. Dynamic contrast-enhanced MRI of gastric cancer: correlations of the pharmacokinetic parameters with histological type, Lauren classification, and angiogenesis. *Magn Reson Imaging* 2017; 37: 27–32.
6 Asahina M, Saito T, Arakawa A, Suehara Y, Takagi T, *et al*. A case of primary spindle cell variant of embryonal rhabdomyosarcoma of the prostate. *Int J Clin Exp Pathol* 2014; 7: 5181–5.
7 Tamada T, Sone T, Miyaji Y, Kozuka Y, Ito K. MRI appearance of prostatic stromal sarcoma in a young adult. *Korean J Radiol* 2011; 12: 519–23.
8 Claikens B, Oyen R, Goethuys H, Boogaerts M, Baert AL. Non-Hodgkin's lymphoma of the prostate in a young male. *Eur Radiol* 1997; 7: 238–40.
9 Andreou A, Whitten C, MacVicar D, Fisher C, Sohaib A. Imaging appearance of sarcomas of the prostate. *Cancer Imaging* 2013; 13: 228–37.
10 Nadal R, Schweizer M, Kryvenko ON, Epstein JI, Eisenberger MA. Small cell carcinoma of the prostate. *Nat Rev Urol* 2014; 11: 213–9.
11 Dixit S, Coup A, Hunt C, Coombs L. Small cell cancer of the prostate. *Urology* 2012; 80: e58–60.
12 Chang JM, Lee HJ, Lee SE, Byun SS, Choe GY, *et al*. Pictorial review: unusual tumours involving the prostate: radiological-pathological findings. *Br J Radiol* 2008; 81: 907–15.

Supplementary Table 1: Clinicopathologic characteristics

Number of patients	*Age (year)*	*Histology*	*PSA (ng ml^{-1})*	*Resenting symptoms*	*Lesion size on MRI (mm)*	*Pathologic access*	*MRI examinations*
1	43	Embryonal rhabdomyosarcoma	0.655	Dysuria	99×98×163	Systematic biopsy	T1WI T2WI DWI
2	22	Embryonal rhabdomyosarcoma	1.668	Dysuria	61×94×63	Systematic biopsy	T1WI T2WI DWI DCE
3	25	Stromal sarcoma	0.471	Dysuria	48×35×40	Open surgery	T1WI T2WI DWI DCE
4	64	Stromal sarcoma	1.937	Dysuria	105×127×120	Open surgery	T1WI T2WI DCE
5	45	Stromal sarcoma	2.50	Dysuria	72×65×75	Open surgery	T1WI T2WI
6	67	Stromal sarcoma	0.97	Dyschezia fresh blood in the feces	50×32×72	Systemic biopsy	T1WI T2WI
7	46	Malignant mesenchymal tumors	0.435	Lower abdominal pain	110×131×166	Systemic biopsy	T1WI T2WI
8	43	Malignant mesenchymal tumors	1.02	None*	80×70×60	Systemic biopsy	T1WI T2WI DCE
9	25	Low-grade sarcoma	2.630	Dysuria	102×111×138	Systemic biopsy	T1WI T2WI DWI, DCE
10	34	Spindle cell sarcoma	1.412	Waist pain perineal pain	72×57 and 78×69	Systemic biopsy	T1WI T2WI DWI DCE
11	63	Small cell carcinoma	5.600	Dysuria	41×21×36	Transurethral resection of the prostate	T1WI T2WI DCE
12	69	Small cell carcinoma	3.140	Dysuria	72×87×90	Systemic biopsy	T1WI T2WI DWI DCE
13	64	Small cell carcinoma	126.634	Dysuria	65×69×77	Systemic biopsy	T1WI T2WI DWI
14	50	Diffuse large B-cell lymphoma	0.522	Lower abdominal pain	93×140×103	Systemic biopsy	T1WI T2WI DWI DCE
15	57	Follicular lymphoma	0.839	None*	54×42×56	Systemic biopsy	T1WI T2WI DWI DCE

*The patient came to the physician for routine physical examination. PSA: prostate specific antigen; MRI: magnetic resonance imaging; T2WI: T2-weighted imaging; T1WI: T1-weighted imaging; DWI: diffusion-weighted imaging; DCE: dynamic contrast-enhanced

Supplementary Table 2: Detailed immunohistochemistry characteristics

Number of patients	*Positive*	*Negative*
1	Myogenin, MyoD1, Ki-67 LI 60%	Desmin, CD117, CD34, DOG1, SMA, S-100, Caldesmon, PCK, EMA, CK8/18, CK19
2	Desmin, Myogenin, MyoD1, Ki-67 LI 60%	
3	Ki-67 LI 40%-50%	PCK, EMA, CK8/18, SMA, Desmin, h-caldesmon, ALK, MyOD1, Myogenin, S-100, HMB45, MelanA, CD34, CD117, DOG1
4	CD117, CD34, DOG1, Caldesmon, Ki-67 LI 6%	SMA, Desmin, S-100, EMA, PCK, MBP
5	VIM	PCK, S-100, Desmin, SMA, CD117
6	CD117, CD34, DOG1, Caldesmon, VIM, Ki-67 LI 10%	SMA, Desmin, S-100, MyoD1, Myogenin, PSA, P504S, P63, HMW-CK, ER, PR
7	VIM, P504S, Syn(+/-), Ki-67 LI 30%	PSA, P63, HMW-CK, PCK, CK8/18, CK19, CK7, CK5/6, CD34, SMA, Desmin, S-100, CgA, EMA
8	SMA, CD10	ALK, Bcl-6, CD20, CD21, CD3, CD30, CD43, CD5, CD56, CD7, CyclinD1, Desmin, GrB, Mum-1, MyoD1, PCK, ER, PR, PSA, S-100, Calponin, Caldesmon
9	VIM, CD99, CD56, Ki-67 LI 10%-20%	PSA, P504S, P63, Syn, CgA, CK7, CK8/18, EMA, PCK, ALK, Desmin, MyoD1, Myogenin, S-100, SMA, LCA
10	VIM, S-100, CD117, Myogenin, Ki-67 LI 50%	CD34, DOG1, SMA, Desmin, PCK, EMA, CK8/18, LCA, MyoD1
11	CgA, Syn, CD56, TTF-1, Ki-67 LI 85%	PSA, P504S
12	CD56, Syn, CgA	PSA
13	PCK, Syn, CD56, P63 ±), Ki-67 LI 80%	CgA, PSA, P504S, HMW-CK, LCA, GATA-3
14	LCA, VIM, CD20, CD79α, CD43, CD10, BCL-2, CD21 and CD23 (FDC+), Ki-67 LI 5%	CD3, CD5, BCL-6, CyclinD1, PCK, PSA, P504s, Syn, CD56, CgA, CD34, PR, ER, SMA
15	VIM, CD20, PAX-5, LCA, MUM-1, ERG, Ki-67 LI 60%	PCK, CK7, CD56, Syn, HMW-CK, PSA, CD3, CD43, CD30, TdT, ALK1, CD138, S-100, CD34, CD31, Desmin, Myogenin, MPO, PLAP, HMB45, SALL-4, CK8/18

CD: cluster of differentiation; DOG-1: discovered on GIST-1; SMA: smooth muscle actin; PCK: pan-cytokeratin; EMA: epithelial membrane antigen; CK: cytokeratin; ALK: anaplastic lymphoma kinase; HMB45: homatropine methybromide 45; MBP: myelin basic protein; VIM: vimentin; PSA: prostate specific antigen; HMW-CK: high molecular weight cytokeratins; ER: estrogen receptor; PR: progesterone receptor; CgA: chromogranin A; syn: synaptophysin; LCA: leucocyte common antigen; bcl-2: B-cell lymphoma-2; PAX-5: the paire box gene 5; MUM-1: multiple myeloma oncogene 1; TTF-1: thyroid transcription factor-1; GATA-3: GATA-blinding protein-3; TdT: terminal deoxynuckotide transferase; MPO: myeloperoxidase; SALL-4: sal-like protein 4; ERG: erythroblast transformation-specific-related gene; GrB: growth factor receptor-bound protein; PLAP: placental alkaline phosphatase

Supplementary Table 3: Magnetic resonance imaging findings

Number of patients	*Shape*	*T2*	*T1*	*DWI*	*Enhancement*	*Pseudo-capsule*	*Cystic change*	*Necrosis*	*Adjacent invasion*	*Metastasis*		
										Bone	*Liver*	*Lung*
1	Irregular	Hyper Iso	Iso Hyper	Hyper	-	Present	Present	Present	Seminal vesical invasion, bladder, and rectal compression	No	No	No
2	Lobular	Hyper	Iso Hyper	Hyper	Heterogeneous	Present	Present	Present	Involving the penis and the right obturator muscle, bladder compression, seminal vesicle intact	No	No	No
3	Lobular	Hyper	Iso Hyper	Hyper	Heterogeneous	Present	Present	Present	Seminal vesical invasion, bladder rectal compression	No	No	No
4	Lobular	Hyper	Iso	-	Heterogeneous	Present	Present	Absent	Seminal vesical invasion, bladder rectal compression	No	No	No
5	Round	Hype Iso	Iso	-	-	Present	Present	Present	Seminal vesical invasion, rectal compression	No	No	No
6	Lobular	Hyper	Iso	-	-	Present	Present	Absent	Seminal vesicle intact, rectal compression	No	No	No
7	Irregular	Hyper	Iso	-	-	Present	Present	Absent	Seminal vesical, rectal and bladder invasion, retroperitoneal nodes metastatic	No	Yes	No
8	Lobular	Hyper	Iso	-	Heterogeneous	Present	Present	Present	Seminal vesical invasion	No	No	No
9	Irregular	Hyper Hypo	Iso Hyper	Hyper	Heterogeneous	Present	Present	Present	Seminal vesical, rectal and bladder invasion	No	No	Yes
10	Lobular	Hype Iso	Iso Hyper	Hyper	Heterogeneous	Absent	Present	Present	Seminal vesical invasion, bladder compression, rectal invasion	No	No	Yes
11	Round	Hype Hypo	Hypo Hyper	-	Heterogeneous	Absent	Absent	Present	Seminal vesical and bladder invasion	Yes	Yes	No
12	Irregular	Hyper	Hypo Hyper	Hyper	Heterogeneous	Absent	Present	Present	Seminal vesical, rectal and bladder invasion	No	No	No
13	Irregular	Hype Hypo	Iso	Hyper	-	Absent	Absent	Present	Seminal vesical and bladder invasion, pelvis lymph node metastases, rectal invasion maybe	Yes	No	No
14	Irregular	Iso	Iso	Hyper	Homogeneous	Absent	Absent	Absent	Seminal vesical, rectal and bladder invasion, pelvis lymph node metastases	No	No	No
15	Round	Iso	Iso	Hyper	Homogeneous	Absent	Absent	Absent	Seminal vesical and bladder invasion, pelvis lymph node metastases	No	No	No

MRI: magnetic resonance imaging; T2WI: T2-weighted imaging; T1WI: T1-weighted imaging; DWI: diffusion-weighted imaging; Hyper: hyperintense; Iso: isointense; Hypo: hypointense; -: none